SITE RESPONSE STUDY OF WEAK AND STRONG GROUND MOTION INCLUDING NONLINEARITY

Feng Su, Yuehua Zeng, John G. Anderson

Seismological Laboratory, University of Nevada-Reno,Reno, Nevada

Vladimir Graizer

California Division of Mines and Geology
Strong Motion Instrumentation Program, Sacramento, California

ABSTRACT

Site response from both weak and strong ground motion recorded at co-located sites were estimated and compared. We find weak and strong motion site responses differ significantly at stations where peak acceleration is above 0.3g, peak velocity is above 20 cm/sec, or shear strain is above 0.06% during the mainshock. The nonlinearity is present across the entire frequency band that we analyzed, from 0.5-14 Hz, and it occurred on sediment sites as well as on soft rock sites. We than compared these observations with a standard engineering model of nonlinear soil response. The model works well for the frequency range from 1.5 to 10 Hz. It diverged from data in frequencies below 1.5 Hz and above 10 Hz, but it is premature to assign much significance to this divergence because the engineering model we used was generic rather than site specific. Finally, we estimated the spectral attenuation parameter Kappa (κ) and compare it between weak and strong motion data at co-located sites. Our result suggests that some of the variability in measurements of κ comes from variability at the source. Kappa may be reduced from weak motion values at sites where nonlinearity is strong, but the source variability has the effect of reducing our confidence in that conclusion.

INTRODUCTION

The recent development of modern seismic instrumentation provides high quality ground motion records from strong motions as well as small earthquakes. This paper aimed to analyze ground response records corresponding to different levels of shaking. Our objectives are (1) to study site response from weak and strong motion including possible nonlinear effects; (2) to examine what we observed from data against a commonly used engineering model for nonlinearity; (3) to evaluate if nonlinear effects modify the spectral attenuation parameter Kappa and if weak motion estimates of kappa are reliable for strong motion.

The Northridge, California earthquake (M_L=6.7) occurred on Jan. 17, 1994. It was followed by hundreds of aftershocks. The mainshock and many of these aftershocks were recorded by the strong motion network stations operated by the California Strong Motion Instrumentation Program (CSMIP). These high quality data provide a unique data set to study weak and strong motion at the same sites. In this study, we have collected seismograms from CSMIP and the SCEC data base at stations with both mainshock and aftershock seismograms.

COMPARISON OF WEAK AND STRONG MOTION SITE RESPONSE AT CO-LOCATED SITES

Site response refers to the highly variable effect of near surface geological structures on the Fourier spectral amplitude of ground motion. In this section of the paper, we summarize the results of Su et al. (1998). They first computed the synthetic Green's function, *G(f,r),* in a regional layered elastic model using an improved reflectivity method of Luco and Apsel (1983). The small event source is treated as a point source with a Brune (1970, 1971) time function. Then the Fourier spectrum of the synthetic Green's function, M(f,r), is

$$M(f,r)=G(f,r)\ \frac{M_0}{\rho\beta^2}\ \frac{(2\pi f)^n}{1+(f/f_0)^2}e^{-\pi\Delta\kappa_s f} \qquad (1)$$

In Equation (1) M_0 is the seismic moment, f_0 is the corner frequency, ρ and β are the material density and S-wave velocity at the source, n is equal to 2 for acceleration seismograms, and $\Delta\kappa_s$ is related to the spectral decay parameter. The Green's function, G(f,r), is computed using a velocity model that includes attenuation along the travel path and in the near surface. The parameter $\Delta\kappa_s$ is an adjustment for the difference between attenuation in the layered crustal model and the site-specific attenuation which may differ. This paper uses a convention that the spectral decay parameter κ is simply measured from the slope of the raw high-frequency acceleration spectrum, as it was defined by Anderson and Hough (1984), and that systematic residuals from a model (as used here or by Anderson, 1991, or Schneider et al, 1993, for example) should be designated as $\Delta\kappa$.

Parameters in Equation (1) that must be adjusted are the seismic moment M_0, the corner frequency f_0, and the attenuation parameter $\Delta\kappa_s$. They are determined for the individual seismograms using the method described by Anderson and Humphrey (1991). That method minimizes the misfit between the spectrum and model by linearizing the fitting for moment and $\Delta\kappa_s$, and systematically testing all plausible values of f_0. The final estimates of seismic moment, $\bar{M}_0$, and corner frequency, $\bar{f}_0$ for each event are obtained by log averaging over the initial estimated M_0 and f_0 from all the stations. Then, we define the reference synthetic spectrum M'(f,r) as

$$M'(f,r)=G(f,r)\ \frac{\bar{M}_0}{\rho\beta^2}\ \frac{(2\pi f)^n}{1+(f/\bar{f}_0)^2}e^{-\pi\overline{\Delta\kappa_s} f} \qquad (2)$$

where $\overline{\Delta\kappa_s}$ is averaged over $\Delta\kappa_s$ from all stations.

The estimate of the site response function from each event is defined as the residual between the logarithms of the observed spectrum, S(f), and the reference synthetic spectrum, M'(f,r). That is,

$$r_s(f)=\log\,[S(f)/M'(f,r)\,] \qquad (3)$$

Since M'(f,r) is the model prediction using the optimal source derived from the observations at several stations, the residual $r_S(f)$ represents the difference in the responses of wave propagation to a particular site compared to wave propagation through the average regional structure. The estimates from several aftershocks are averaged to obtain the final estimates for weak motion site response at each station.

The strong-motion site response was estimated by the spectral ratio of the observed strong ground motion to the synthetic seismogram calculated using the composite source model in the same layered crustal sturcture, and with the same correction for $\Delta\kappa_s$, as that used in the weak motion estimation.

Using the above methods, Su et al (1998) estimated weak and strong motion site response functions from the Northridge mainshock and its aftershocks. Figure 1 shows the location of the weak and strong motion stations and events we used in site response estimation. Information about these weak and strong motion stations is also listed in Table 1. Figures 2a and 2b compare strong motion with weak motion site response functions for the horizontal and vertical components, respectively. Both strong and weak motion site amplification were normalized to a rock station LA00 before taking the ratio to further eliminate any source bias in the strong motion site response estimation. This normalization implies an assumption that the nonlinear site response at station LA00, if there is any, is negligible. LA00 is situated on a Mesozoic rock site south of the fault and away from the rupture direction. Thus, we considered it the best choice for a station that is unlikely to be strongly affected by either details of the rupture model or nonlinear site response. In the end, this means that the Greens' functions *G(f,r)* have been used to make a more sophisticated adjustment for geometrical spreading than simpler assumptions such as (1/r) that have been used in some other studies of site response for widely distributed stations.

Figure 2b shows that for the vertical component, the weak and strong motion site responses generally agree. In contrast, for the horizontal components (Figure 2a), the weak motion site responses are almost never smaller than the strong motion responses, and often the weak motion response is greater. The difference between weak and strong motion site response is most significant at stations TAG, JFPP and NWHP.

To quantify the difference between weak and strong motion site response, we define the average strong to weak motion ratio, *ASW Ratio*, as

$$ASW\ \ Ratio = \exp\left\{\frac{1}{N_f}\sum_{i=1}^{N_f}\ln\left(\frac{r_S(f_i)}{r_W(f_i)}\right)\right\} \qquad (4)$$

where $r_s(f_i)$ is the strong motion site response function and $r_w(f_i)$ is the weak motion site response function, after normalization to response at station LA00. Only the horizontal component of the site response function is considered. N_f is the total number of the frequency points used in the average. The frequencies are equally spaced on a logarithmic scale over the frequency band from about 0.5 Hz to about 14 Hz.. Here we used the ASW Ratio instead of the AWS Ratio, the

inverse of the ratio in Equation (4) used by Su et al. (1998), to consistent with what the engineer used discussed later.

The solid circles in Figures 3a, b and c give *ASW Ratio* as a function of the peak ground acceleration (PGA), peak ground velocity (PGV), and shear strain (e_{max}) observed at each station during the main shock, respectively. The values of PGA and PGV are obtained from the seismograms of the mainshock. For a general solution to the wave equation in a homogeneous medium, the strain is equal to the ratio of particle velocity to medium velocity. Thus, we estimate e_{max} as $e_{max}=(PGV/v_s)$ where v_s is the average shear velocity in the upper 30 meters at the site. The v_s is estimated from the generalized geology at each site according to Park and Elrick (1998). To be specific, we uses v_s equal to 332 m/s, 397 m/s, and 569 m/s for Quaternary, Tertiary, and Mesozoic sites, respectively.

If site responses from strong and weak motion are about the same, the *ASW Ratio* will be close to unity. In Figure 3, at stations with relatively low amplitudes of ground motions, the *ASW Ratio* is near unity, indicating that the strong and weak motion site response functions agree with each other within the uncertainty. However, the *ASW Ratio* decreases as the recorded peak motions increase, indicating there is a deamplification effect in strong motion compared to weak motion. When the recorded peak acceleration is greater than about 0.3g, peak velocity is greater than about 20 cm/sec, or shear strain is greater than about 0.06%, this strong motion deamplification effect becomes significant. There could be some nonlinearity in the stress-strain relationship at smaller amplitudes, but the effects of nonlinearity are emerging from the other uncertainties and becoming significant for ground motions above the threshholds identified here.

Figure 3 shows direct evidence of nonlinearity at the sites with the higher levels of ground motions. It demonstrates a relationship between nonlinear site response and peak ground acceleration, peak ground velocity, and shear strain. The nonlinearity is not only present in sediment sites but also on soft rock sites like TAG and LA01(see Table 1 for their site condition and *ASW Ratio*). This is not surprising in the context of laboratory studies which find nonlinearity of rock samples (Johnson and McCall, 1994, Johnson and Rasolofosaon, 1996).

Figure 3 suggests a threshold in peak acceleration, peak velocity, and peak strain that can be used in several ways. Whenever an observation exceeds the threshold, nonlinear site response should be anticipated. Whenever linear calculations predict ground motions that exceed the threshold, reevaluation using nonlinear methods is necessary. Finally, these results can be used to test the commonly used nonlinear models. That is, when these calculations are performed, a linear calculation can also be carried out, and the ratio would be expected to consistent with Figure 3. This is discussed in next section.

To investigate this nonlinear site response in the frequency domain, we examined the ratios of strong to weak motion site amplification as a function of frequency and averaged the ratios over the stations. This average, obviously, has no particular meaning since it depends on the distribution of stations. It takes on meaning when, for a group of strongly shaken stations, it has an average that differs from unity. Figure 4 shows the averaged ratio (thick line) over 15 sediment stations we studied. Its 95% confidence zone is indicated by the green shades. On average, the ratio is equal to 0.6, meaning the average site deamplification during earthquake

strong motion is about 0.6 times those of weak motions. This deamplification is significant and it occurred across the entire frequency band we studied, implying nonlinearity is present at all these frequencies.

COMPARISON OF THE OBSERVATIONS WITH AN ENGINEERING MODEL PREDICTION

A typical approach to simulating nonlinear soil response is to estimate the effects of nonlinear wave propagation through a stack of sediments. For this, following Ni et al (1997), we chose a time-domain wave propagation model of Lee and Finn (1978). In this model, the entire seismogram is treated as a vertically-propagating shear wave that excites the stack of sediments from the bottom. The calculations can be performed either assuming linear elastic response of the sediment or assuming the sediments follow a non-linear stress-strain relationship that obeys the Masing rule (1926). The shape of the nonlinear stress-strain relationship is controlled by a "modulus reduction curve" that gives the average secant shear modulus as a function of the strain. A model of modulus reduction curves, which includes the effects of both confining pressure (depth) and rigidity, has been presented in EPRI(1993), and is used as the input for our calculations.

A common site model was used for all sites. It has a mean shear wave velocity of 370 m/s for the upper 30 meters (Park and Elrick, 1998) with a water table at 3 meters below the surface. The total thickness of the soil column is 100 meters. Test runs suggest that the simulation result become less dependent on the depth of the sediments when the thickness of the soil column is greater than 60 meters.

We then generated over 1000 synthetic accelerograms for a dense distribution of stations surrounding the Northridge area. These were generated using the composite source model (Zeng et al, 1994). Assuming the linear response of the soil column represents the weak motion site amplification and its nonlinear response represents the strong motion site amplification, we computed the same *ASW Ratio* from each station and plotted them on Figure 5. The general trends of *ASW Ratio* as a function of peak acceleration (figure 5a) are similar between model and observation, although the model falls off a little less rapidly than the data, especially for the peak velocity (figure 5b) and strain (figure 5c). The synthetics also show less scatter than the data.

To compare nonlinear response in the frequency domain between the model and the data, we used site specific synthetic predictions as input to generate synthetic accelerograms under both linear and nonlinear approaches at the 15 sediment sites. Following a similar procedure as used for the data, we calculated the ratio of strong (nonlinear) to weak (linear) motion site response for each site, and then averaged it over the 15 sites included in Figure 4. In Figure 6 the synthetic average is plotted with the data for comparison. The results show that the model matches well with the data in the frequency range from about 1.5 to 10 Hz. However, they diverge at frequencies below 1.5 Hz and above 10 Hz. At frequencies above 10 Hz, the model shows a rapid increase in amplitude ratio, up to a factor of two for nonlinear response in comparison with linear response at about 14 Hz. This is a model artifact due to the nonlinear stress-strain relation, which produces a sudden change in shear modulus as the shear strain reverses. At frequencies below 1.5 Hz, the amplitude ratio from data is significantly different

from unity, although it shows a trend of convergence to unity. In contrast, the synthetic ratio is essentially equal to unity. The departure of the synthetics from the data below 1.5 Hz is the cause of a less rapid fall off in the synthetics for the *ASW Ratio* versus ground motion parameters (Figure 5), especially for peak velocity or strain, since the ground velocity pulses are dominated by lower frequency waves than that of the ground acceleration.

In order to check if the low amplitude ratio measured from data for frequencies 0.5 to 1.5 Hz is real, we carefully examined the data to be certain that signals are significantly above noise levels. In addition, our site response functions were normalized to the rock station LA00 so the source effect from mainshock and aftershocks is minimized. Our result of the observed nonlinearity presented at all frequencies studied is also consistent with the result by Field et al (1997) who referenced their site amplifications to the average of several rock sites. A recent work by Cultrera et al. (1998) on the site responses at the Jensen Filtration Plant shows that the weak motion records of aftershocks within two minutes of the mainshock exhibit a nonlinear deamplification comparable to that of the mainshock, suggesting that the nonlinear shear modulus reduction that occurred during strong shaking may not recover back as quickly as the current engineering model predicts. Thus the longer period and relatively lower amplitude motion will experience the same nonlinear deamplification as that of the high frequency waves. As a consequence, the observed ground motion suffers further amplitude reduction than the model prediction.

It is premature to assign much significance to the disagreement of the model with the observations at low and high frequencies. One hypothesis is that there is a problem with the way that the nonlinearity is modeled. A nonlinear reduction in low frequencies could result from a delay in recovery of the shear modulus reduction after strong shaking. However, we used a generic soil model which we applied to all of the stations. Detailed models at each of the stations would undoubtedly differ even if the average velocity for the station is the same. For instance, one way that the detailed models would likely differ is by having alternating layers of higher and lower velocities; in this case nonlinearity in the low velocity layers could have a stronger effect on the low frequency waves than what is predicted by a model in which these layers are absent. It will be important to test the difference between the linear and nonlinear response with the specific site characteristics that are being developed in the ROSRINE project in future investigation.

SYNTHETIC SEISMOGRAMS INCORPORATING NONLINEARITY

Eventually, it is our hope that the models for generating synthetic seismograms might be so good that they can replace regression analysis. The results of the above sections strongly suggest that it is necessary to incorporate nonlinearity into these models in a systematic way when computing ground motions at short distances.

We undertook to test how well our synthetic seismogram model performed for the Northridge case. The model was tested previously by Anderson and Yu (1996) in a blind prediction and the resulting ground motion prediction is consistent statistically to the observation. Zeng and Anderson (1996) demonstrated that a specific realization of the composite source is capable of matching waveforms at low frequencies. For this study, we

carried out an experiment closer to that of Anderson and Yu (1996). Our parameters were not generated using a blind test as they did, but rather picked to be consistent with the source parameters used by Zeng and Anderson. We used a different regional velocity model and a different Q model that has subsequently been demonstrated to be more appropriate. Synthetics were passed through the generic nonlinear soil model as described above.

Our initial set of accelerograms showed a higher amount of directivity at high frequencies than we considered to be realistic. Motivated by the fact that we do not observe any distinct radiation pattern and wave polarization at high frequency, we therefore introduced an effective high frequency source radiation term. This source radiation consists of energy contributions from an angular cross section centered at the direction from the source to receiver in order to simulate high frequency wave reflection and scattering at the fault zone. The total source radiation then equals

$$b*\textit{effective-source-radiation} + (1- b)*\textit{double-couple-source-radiation} \qquad (5)$$

where b is a continuos function of frequency. It equals 1 above a high frequency threshold and tapers to 0 at low frequency since this reflection and scattering at the source zone has less an effect at lower frequencies.

This modification to the composite source model was validated with the Northridge strong motion observations. Figure 7 gives examples of the nature of the observed ground motions and the model predictions. Figure 8 compares the results of this improved method and that of a regression prediction (Abrahamson and Silva, 1997) to the observed PGA and to SA at a period of 3 second. Our synthetics as modified by Equation (5) predict the trends of the observed ground motion parameters better than the regression. The figures also show the standard errors of prediction from the improved composite source model and from the Abrahamson and Silva's regression. For comparison, without the modification in Equation (5), the standard errors in prediction PGA increased from 0.455 to 0.554, and for predicting SA at a period of 3 second increased from 0.65 to 0.66. Since the modification is to simulate near source scattering effect at high frequency, the improvement high frequency simulation is expected. The scatter in the data is caused in part by the local site and basin response effects which are not modeled in the current context of high frequency simulation.

COMPARISON OF THE SPECTRAL ATTENUATION PARAMETER KAPPA MEASURED FROM WEAK AND STRONG MOTION RECORDS

The parameter kappa (κ) was defined by Anderson and Hough (1984) to describe the shape of the high frequency spectrum of accelerograms. The study was actually motivated in part by an earlier paper by Hanks (1982) recognizing that the acceleration spectrum falls off rapidly at high frequencies. Anderson and Hough observed that the high-frequency acceleration spectrum falls off approximately exponentially with frequency, i.e. $A(f) \sim \exp(-\pi\kappa f)$. Based on observations at a single station, they found that κ increased with distance from the earthquake, but that the intercept of that trend varied from one station to another. Based on this observation they proposed that the most reasonable explanation for the systematic behavior of the parameter kappa was that the parameter was caused by attenuation. They suggested that the

attenuation had a strong contribution from site conditions, but that it also had a contribution from regional wave propagation. Anderson (1991) attempted to generalize the model, describing the observations of κ in southern California from Anderson and Hough (1984), Hough et al (1988), and Hough and Anderson (1988) with the model:

$$\kappa = \kappa_0 + \tilde{\kappa}(r) \qquad (6)$$

where the term κ_0 was conceived of as predominantly a site term and $\tilde{\kappa}(r)$ characterized the distance dependence. The relationship between κ and the seismological measure of energy loss, Q, is not straightforward. The normalization of κ is the same as the normalization of t^*, which is directly related to Q ($t^*=r/(Qv_s)$), but as pointed out first by Anderson and Hough (1984) and Anderson (1986), κ will only equal t^* if Q is independent of frequency. Many observations exist suggesting a frequency dependence of Q. This difficulty, however, does not seem to severely limit the usefulness of κ to characterize the acceleration spectrum at high frequencies, since κ is defined as an observational parameter.

Anderson (1986) pointed out the implications of this model for small earthquakes: if the small earthquake spectrum is affected the same way as the strong motion spectrum, distinguishing between the effects of the source and the attenuation would become difficult for smaller events as the corner frequency moves into the high frequency band where κ is measured. To overcome this difficulty Anderson and Humphrey (1991) proposed a method to measure κ relative to a Brune (1970) model for the spectrum of small events. This method was applied by Humphrey and Anderson (1992) and Su et al (1996) with apparent success. Schneider et al (1993) point out the usefulness of the parameter κ for predicting strong motions from future events, so it is important to be able to estimate κ for the site without waiting for a strong earthquake to occur. However, considering differences in the earthquake sources and particularly the potential importance of nonlinear site response, it is important to check how well measurements of κ from small events predict κ at the same site during large events. In this study, we use some of the excellent CSMIP data to make this comparison.

This comparison is particularly timely due to some studies on κ in southern Nevada. Estimates of κ by Biasi and Smith (1997) from extremely small earthquakes, still assuming a Brune spectral shape with a stress drop similar to the stress drop of larger events, gave values of κ that were larger than those obtained by Su et al (1996). Furthermore, both of these studies showed a larger amount of scatter in estimates of κ that one would expect for a parameter dominated by wave propagation.

We examine κ from two data sets in southern California. First, we examine κ from weak and strong motions for the data set used by Su et al (1998). Secondly, we examine it from a subset of the strong motion records of Northridge aftershocks recorded on CSMIP instruments. For both data sets, we assumed that the distance-dependent term can be linearized over the short distance range used in this data as $\tilde{\kappa}(r) = ar$. Then, we have

$$\kappa = \kappa_0 + ar \qquad (7)$$

where a is related to the Earth's velocity and Q structure and r is the hypocentral distance. Conceptually, a would equal $1/(QsVs)$ if Q_S were independent of frequency.

In the study of the aftershock data used in Su et al (1998), we measured κ in the frequency band of 5 to 20 Hz. The analysis procedure was somewhat different from the approach described by Equations 1-4, instead following the approach used by Su et al (1996) for small events in southern Nevada. Once the basic measurement of κ was obtained from each seismogram, we used a least-squares method to determine the constants a and an average value of κ_0 for each station from weak motion data. In this case, we obtained a=0.00136 *s/km.* For strong motion data, we measured the slope of the accelerograms directly (as in Anderson and Hough, 1984), and adjusted the slope for distance using the same constant a. In addition to the data used by Su et al (1998), we used CSMIP aftershock data from two closely spaced stations at Tarzana, that is, the station at Cedar Hills Nursery (NUR) and Clubhouse (CLU). The two stations are about 150 meters apart. Figure 9 shows the locations of the Tarzana stations and the events we used. In this case also, κ was measured directly from the S-wave spectrum of the accelerogram. Figure 10 shows these spectra and the spectral fits that produce the individual κ measurements.

If the estimates of κ_0 are to be usefully compared between weak and strong motion records, then it is critical that the distance correction must be reliable. For that reason, before presenting the data, we test the distance correction for the second set of data. For an individual observation, we calculate κ_0^i with the equation:

$$\kappa_0^i = \kappa - ar \qquad (8)$$

Obviously, if the model behind Equation (7) holds, then κ_0^i should be the same for every observation, and that constant would be recognized as the site term κ_0. The distance correction in Equation 8 can be considered if the individual estimates of κ_0^i are independent of distance.

For this purpose, Figure 11a shows the individual estimates of κ and of κ_0^i versus distance for the value of a for the station NUR and Figure 11b for the the station CLU. The raw measurements of κ show a rather strong distance dependence. After correction, κ_0^i is not correlated with distance, indicating that a is reasonable. This value of a is larger than the value estimated by Anderson and Hough (1984) for the same region. The difference is that in this case, the distances are smaller, and the path is therefore expected to be much shallower. The smaller value of a is expected from a depth dependence to Q.

Figure 12 shows κ_0^i estimated from 21 main shock accelerograms (solid circle) used by Su et al (1998) and the station average for weak motion (open circle) at the same stations. These are plotted against the observed PGA during the mainshock. This figure indicates that κ_0^i from weak and strong motion data are not simply the same. For peak accelerations in the range where nonlinearity is present, i.e. above 0.3g (Fig. 3), most of the values of κ_0^i from the weak motions are greater than the corresponding value for the strong motion record. A reduction in kappa for strong motion records is in the same direction as the predictions of Yu et al (1993) and Ni et al (1997), although those papers may predict a greater difference than what is observed.

Figure 13a compares unadjusted estimates of κ at the adjacent Tarzana stations, NUR and CLU, and Figure 13b compares the estimates of κ_0^i between the two stations. The unadjusted estimates of κ are strongly correlated, but this is to be expected since the differences in hypocentral distances are significant for different aftershocks. The residuals after adjusting for distance, the various estimates of κ_0^i, have a smaller range, but the residuals are still correlated.

It seems most likely that the correlation is related to the earthquake source in some generalized way. The residuals are not related to the source depth as we have checked. However, Several other source parameters might be hypothesized to have an impact. One is the source spectral shape, which may have some variation in the high-frequency rolloff A second possibility is that there is some dependence of κ on the radiation pattern at the source. The take-off angles to the two Tarzana stations are probably nearly identical for each event, but are expected to be sampling different sections of the radiation pattern for different events. Another possibility is that the residual is associated with some local anomaly in attenuation or scattering in the vicinity of the source. With the data used in this study, it is not possible to distinguish among these possibilities.

The significance of this result is that the spectral decay parameter is affected by more physical phenomena than that presented in Equations (6) and (7). Figure 12 suggests that nonlinear site response might cause κ to be decreased. Figure 13 suggests that the source of moderate-sized earthquakes affects the spectral decay at high frequencies. Equations (6) and (7) may need to be modified by the addition of a source term. Both Figures 12 and 13 indicate that some caution is needed in extrapolating from values of κ_0 estimated from small earthquakes to the value expected in large events.

CONCLUSION

In summary, nonlinearity appears to have decreased the average amplitudes of ground motions at sites that experienced the strongest shaking in the Northridge earthquake across the entire frequency band from 0.5-14 Hz. The data indicate that the nonlinearity was present when the peak acceleration exceeded 0.3g, the peak velocity exceeded 20 cm/sec, or the peak strain exceeded 0.06%. A comparison of these observations with a standard engineering model of nonlinear soil response indicates that the model works well for the frequency range from 1.5 to 10 Hz. However, the model diverged from data in frequencies below 1.5 Hz and above 10 Hz. At frequencies below 1.5 Hz, the data show continuous nonlinear deamplification in contrast to the model prediction. At frequencies above 10 Hz, the model generated additional high frequency energy which is actually an artifact of the nonlinear stress-strain relationship used. Nevertheless, the average model improves predictions of synthetic seismograms to the point where they are comparable to predictions of regression equations. Our result suggests that some of the variability in measurements of the spectral attenuation parameter κ comes from variability at the source, in contrast to the models in which κ is controlled entirely by path and site effects. Our results also suggest that κ measurements may be affected by nonlinear site response.

REFERENCES

Anderson, J. G. (1986). Implication of attenuation for studies of the earthquake source, Earthquake Source Mechanics, Geophysical Monograph 37, (Maurice Ewing Series 6), American Geophysical Union, Washington, D.C. 311-318.

Anderson, J.G. (1991). A preliminary descriptive model for the distance dependence of the spectral decay parameter in southern California, Bulletin of the Seismological Society of America 81, 2186-2193.

Anderson, J. G. and S. Hough (1984). A Model for the shape of the Fourier amplitude spectrum of acceleration at high frequencies: Bull. Seism. Soc. Am. 74, 1969-1994.

Anderson, J. G. and J. R. Humphrey, Jr. (1991). A least-squares method for objective determination of earthquake source parameters, Seismological Research Letters, 62, 201-209.

Anderson, J. G. and G. Yu, Predictability of strong motions from the Northridge, California, Earthquake. Bull. Seism. Soc. Am. 86, S100 (1996).

Biasi, G. P. and K. D. Smith (1997). Project report: site effects for seismic monitoring stations in the vicinity of Yucca Mountain, Nevada, WBS#1.2.3.2.8.4.1, Task #SPT38BM4.

Brune, J. N., Tectonic stress and the spectra of seismic shear waves from earthquakes from earthquakes, J. Geophys. Res. 75, 4997 (1970).

Brune, J. N., Correction, J. Geophys. Res. 76, 5002 (1971).

Cultrera, G., D. M. Boore, W. B. Joyner and C. M. Dietel, Nonlinear soil response in the vicinity of the Van Norman Complex following the 1994 Northridge, California, earthquake, Submitted to Bull. Seism. Soc. Am. (1998).

EPRI, Guidelines for determining design basic ground motions. Volume 1: Method and guidelines for estimating earthquake ground motion in Eastern North America, report, EPRI TR-102293, Nov. (1993).

Lee, K. W. and W. D. L. Finn (1978). DESRA-2: dynamic effective stress response analysis of soil deposit with energy transmitting boundary including assessment of liquefaction potential, *Soil Mechanics Series*, University of British Columbia, Vancouver, Canada.

Field, E. H., P. A. Johnson, I. A. Beresnev and Y. Zeng, Nonlinear sediment amplification during the 1994 Northridge earthquake, Nature, 599 (1997).

Frankel, A., High-frequency spectral falloff for earthquakes, fractal dimension of complex rupture, b-value, and the scaling of strength on faults, J. Geophys. Res., 96, 6291 (1991).

Gao, S., H. Liu, P. M. Davis, and L. Knopoff, Localized amplification of seismic waves and correlation with damage due to the Northridge earthquake: evidence for focusing in Santa Monica, Bull. Seism. Soc. Am. 86, S209 (1996).

Hanks, T. C. (1982) fmax, Bull. Seism. Soc. Am 72, 1867-1880.

Hough, S.E. and J. G. Anderson (1988). High-frequency spectra observed at Anza, California: implications for Q structure, Bull. Seism. Soc. Am. 78, 692-707.

Hough, S. E., J. G. Anderson, J. Brune, F. Vernon III, J. Berger, J. Fletcher, L. Haar, T. Hanks and L. Baker (1988). Attenuation near Anza, California, Bull. Seism. Soc. Am. 78, 672-691.

Humphrey, J. R. Jr. and J. G. Anderson (1992). Shear wave attenuation and site response in Guerrero, Mexico, Bulletin of the Seismological Society of America 82, 1622-1645.

Johnson, P. A. and K. R. McCall, Observation and implications of nonlinear elastic wave response in rock, Geophy. Res. Let., 21, 165 (1994).

Johnson, P. A. and R. N. J. Rasolofosaon, Manifestation of nonlinear elasticity in rock: convincing evidence over large frequency and strain intervals from laboratory studies, Nonlinear Processes in Geophysics, 3, 77 (1996).

Lee, K. W. and D. L. Finn, DESRA-2: Dynamic effective stress response analysis of soil deposit with energy transmitting boundary including assessment of liquefaction potential, Soil Mechanics Series, University of British Columbia, Vancouver, Canada (1978)

Masing, G., Eigenspannungen und Verfestigung beim Messing, proceedings, 2nd International congress of Applied Mechanics, Zurich (1976).

Ni, S.-D., R. V. Siddharthan and J. G. Anderson (1997). Characteristics of nonlinear response of deep saturated soil deposits, Bull. Seism. Soc. Am. 87, 342-355.

Park, S. and S. Elrick, Predictions of shear-wave velocities in southern California using surface geology, Bull. Seism. Soc. Am. 88, 677 (1998)

SCEC phase III report. (1998).

Schneider, J. F., Silva, W. J., and C. Stark (1993). Ground motion model for the 1989 M 6.9 Loma Prieta earthquake including effects of source, path, and site, Earthquake Spectra 9, 251-___.

Su, F., J. G. Anderson, J. N. Brune, Y. Zeng (1996). A comparison of direct S-wave and coda wave site amplification determined from aftershocks of the Little Skull Mountain earthquake, Bull. Seism. Soc. Am. 86, 1006-1018.

Su, F., J. G. Anderson and Y. Zeng, Study of weak and strong ground motion including nonlinearity from the Northridge, California, Earthquake sequence, Bull. Seism. Soc. Am, in press (1998)

Su, F., Y. Zeng, and J. G. Anderson, Simulation of the Loma Prieta earthquake strong ground motion using a composite source model, EOS, 75, 448 (1994).

Yu, G., J. G. Anderson, R. Siddharthan (1993). On the characteristics of nonlinear soil response, Bull. Seism. Soc. Am., 83, 218-244

Yu, G., K. N. Khattri, J. G. Anderson, J. N. Brune and Y. Zeng (1995). Strong ground motion from the Uttarkashi, Himalaya, India earthquake: comparison of observations with synthetics using the composite source model, Bull. Seism. Soc. Am. **85**, 31-50.

Zeng, Y., J. G. Anderson and F. Su, Subevent rake and random scattering effects in realistic strong ground motion simulation, Geophy. Res. Lett. , 22, 17 (1995).

Zeng, Y., J. G. Anderson and G. Yu, A composite source model for computing realistic synthetic strong ground motions, Geophy. Res. Lett, 21, 725 (1994).

Zeng, Y. and J. G. Anderson, A composite source model of the 1994 Northridge earthquake using genetic algorithms, Bull. Seism. Soc. Am. 86, S71 (1996).

Table 1: Station Information

Name	Location (Latitude, Longitude)		NE[a]	Strong-motion Station (source[b]-site name)	PGA[c] (cm/s²)	PGV (cm/s)	ASW Ratio		Site Geology[d]
CPCP	34.2114	-118.6081	11	USC-station #53	320	28.7	0.48	Q	sediment
JFPP	34.3120	-118.4960	9	USGS-Jensen Filter Plant	416	40.8	0.25	Q	sediment
KSRG	34.0596	-118.4736	11	USGS-LA, Brentwood VA Hosp.	143	14.9	1.02	Q	sediment
LA00	34.1062	-118.4542	20	SCEC-Stone Canyon Reservoir	307	24.1	1.00	M	hard rock
LA01	34.1317	-118.4394	16	USC-station #13	388	36.2	0.43	T	soft rock
LA03	34.0900	-118.3390	9	CDMG-LA, Hollywood Storage Bldg.	256	15.1	0.97	Q	sediment
LA04	34.0700	-118.1500	6	CDMG-Alhambra, Fremont School	81	5.4	1.01	Q	sediment
MKDR	34.2173	-118.5235	7	USC-station #3	355	26.3	0.39	Q	sediment
MPKP	34.2871	-118.8816	10	CDMG-Moorpark	221	16.0	0.73	Q	sediment
NHFS	34.1988	-118.3978	13	USC-station #9	258	14.8	0.81	Q	sediment
NWHP	34.3880	-118.5332	16	CDMG-Newhall	540	60.2	0.22	Q	sediment
OVHS	34.3285	-118.4460	3	CDMG-Sylmar County Hosp.	594	45.9	0.64	Q	sediment
PDAM	34.3341	-118.3980	10	CDMG-Pacoima Dam Downstream	369	27.0	1.07	M	hard rock
SFYP	34.2369	-118.4391	5	CDMG-Arleta	256	22.3	0.58	Q	sediment
SMC	34.0122	-118.4913	5	CDMG-Santa Monica City Hall	498	23.5	0.69	Q	sediment
SMIP	34.2632	-118.6673	6	USC-station #55	475	41.4	0.40	T	sediment
SSAP	34.2309	-118.7135	13	USGS-Santa Susana	234	11.8	0.74	M	hard rock
SSC	34.0467	-118.3557	9	USC-station #91	395	28.8	0.76	Q	sediment
TAG	34.1604	-118.5343	6	CDMG-Tarzana	1150	61.4	0.20	Q	soft rock
VAN	34.2493	-118.4777	8	USGS-LA, Sepulveda VA Hosp.	706	59.5	0.46	Q	sediment
WVES	34.0050	-118.2790	3	USC-station #22	251	17.7	1.15	Q	sediment

a: Number of aftershock events used at that station.

b: The source of strong motion data is as follows: USC - University of Southern California; SCEC - Southern California Earthquake Center; CDMG - California Division of Mines and Geology; USGS - United States Geological Survey.

c: PGA and PGV are the arithmetic averages of the peak ground acceleration and velocity of two horizontal components, respectively. The seismograms were filtered in frequency band of 0.1 - 15.0 Hz in time doman before obtaining peak values.

d: M=Mesozoic and older rocks, T=Tertiary sediments, Q=Quaternary sediments. The averaged shear wave velocity in the upper 30 meters is 333m/s for Quaternary sediments , 406m/s for Tertiary and 589m/s for Mesozoic according to Park and Elrick (1998).

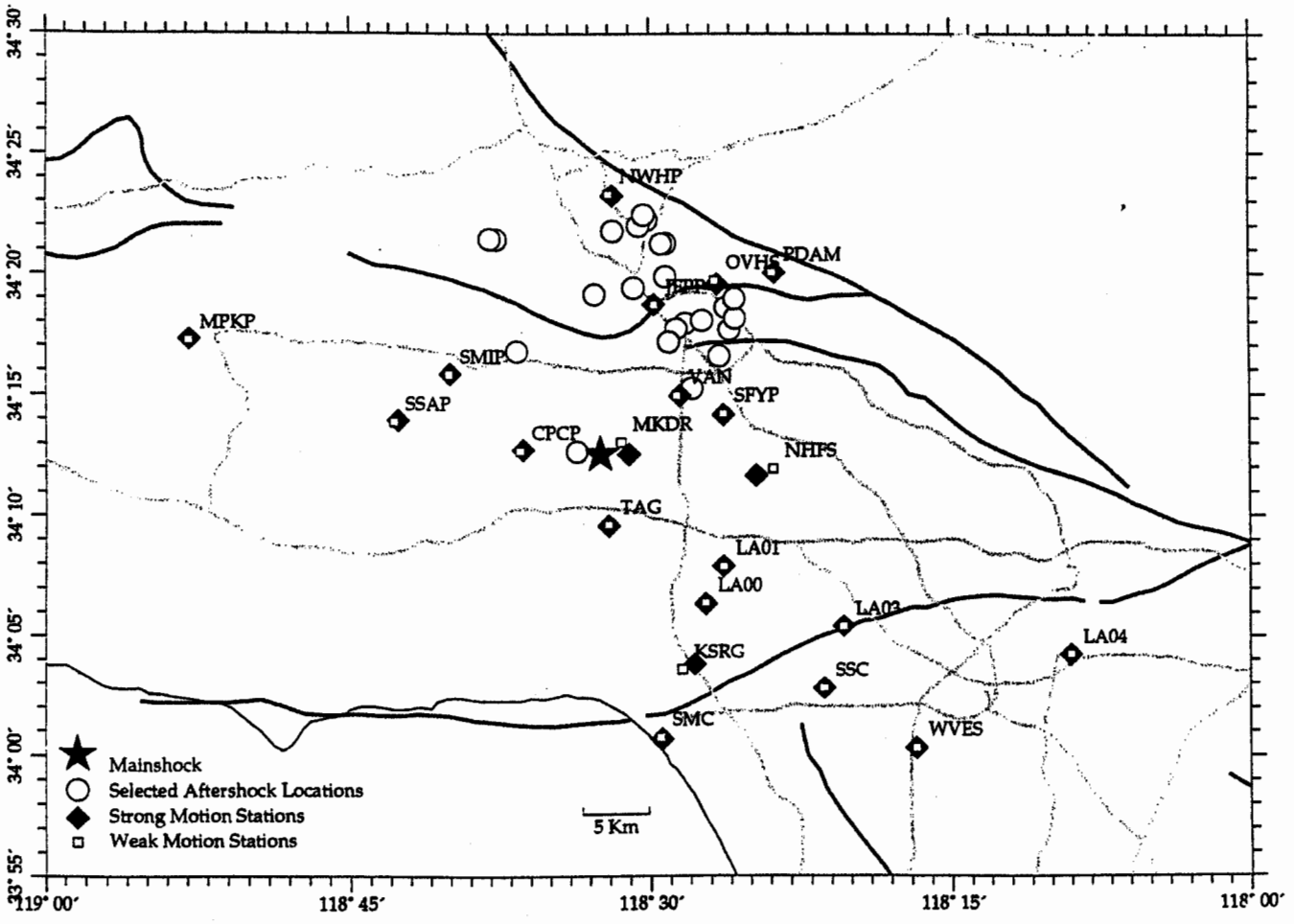

Figure 1: Map view of the event and station distributions used in this study.

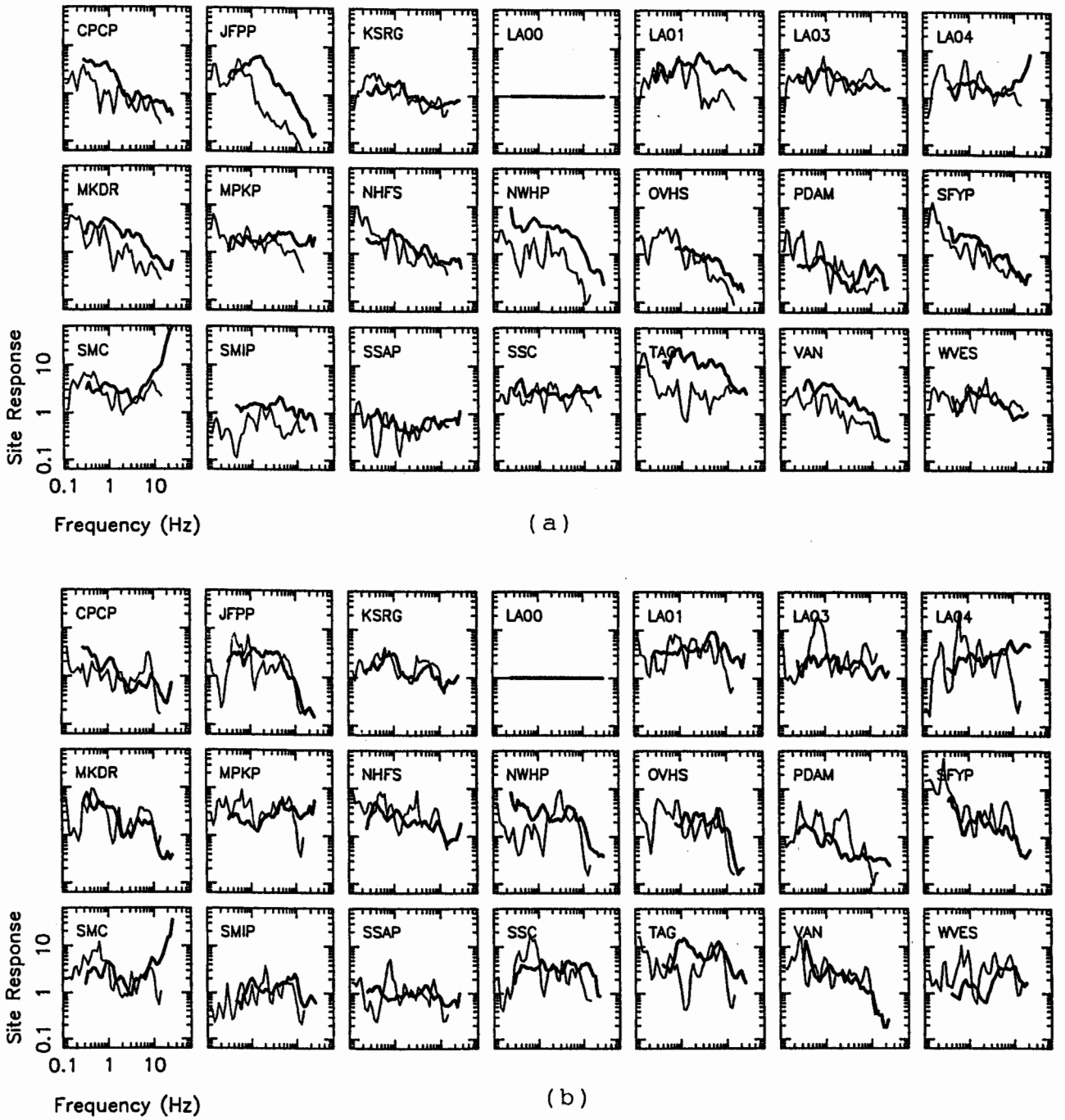

Figure 2: Comparisons of weak and strong motion site amplifications at their co-located sites. The thick and thin lines represents the site amplification obtained from weak motion and strong motion data, respectively. (a) Average of the horizontal components. (b) Vertical component.

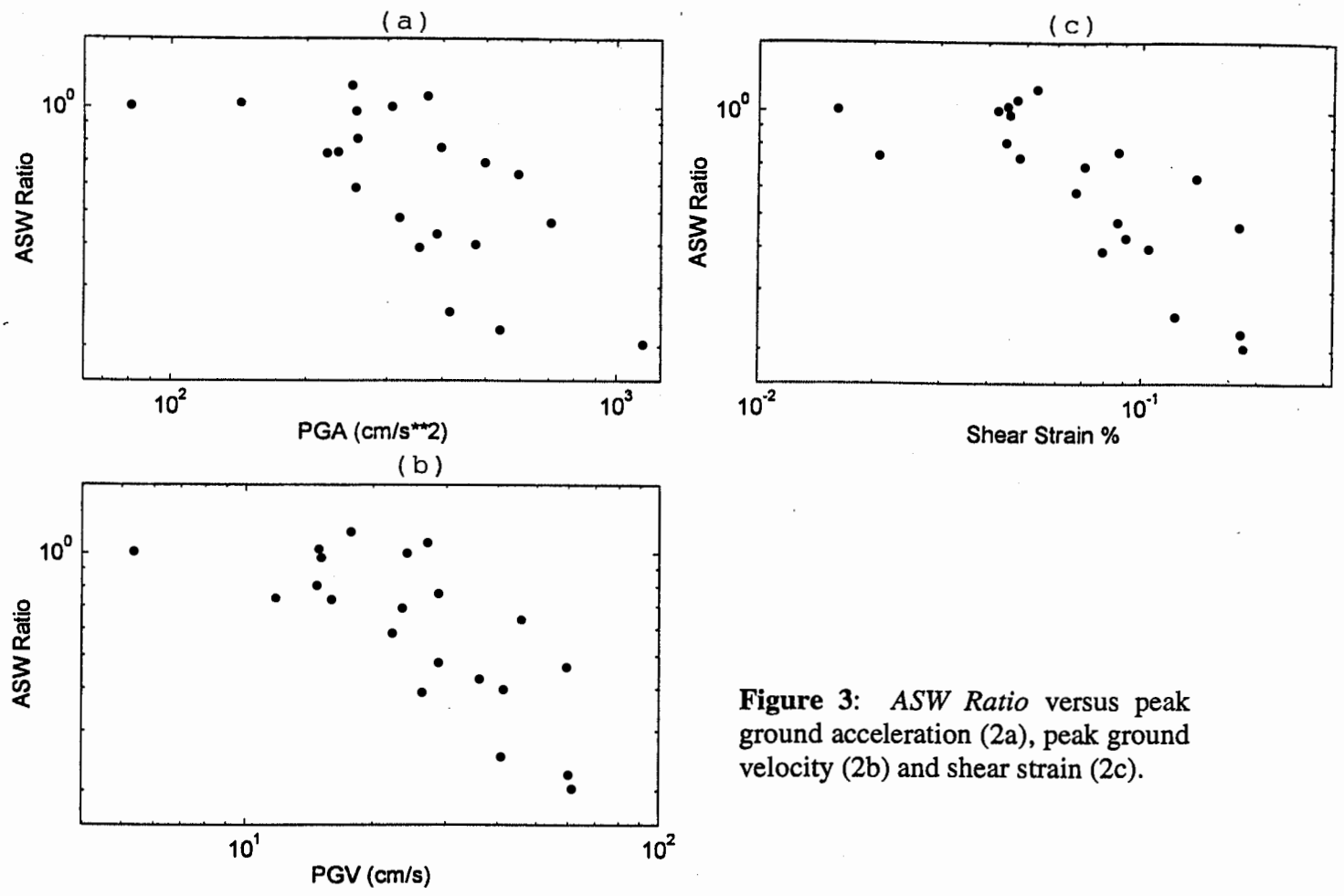

Figure 3: *ASW Ratio* versus peak ground acceleration (2a), peak ground velocity (2b) and shear strain (2c).

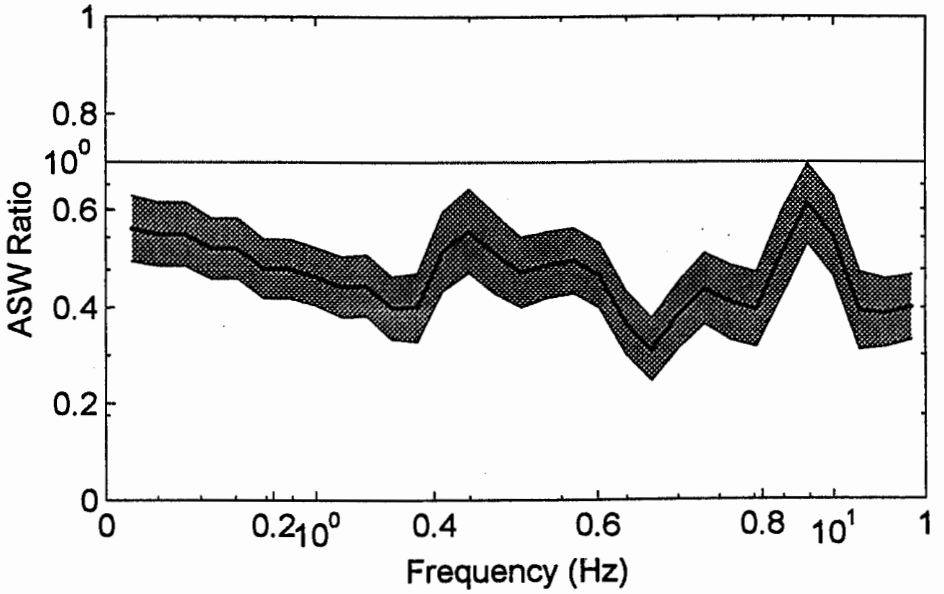

Figure 4: Ratio of strong to weak motion site response versus frequency averaged over 15 sediment sites we used (see Table 2 for station site condition. Station SMC is excluded since it may have focusing effect due to subsurface structure according to Gao et al. (1996)). The shaded area indicates the 95% confidence zone.

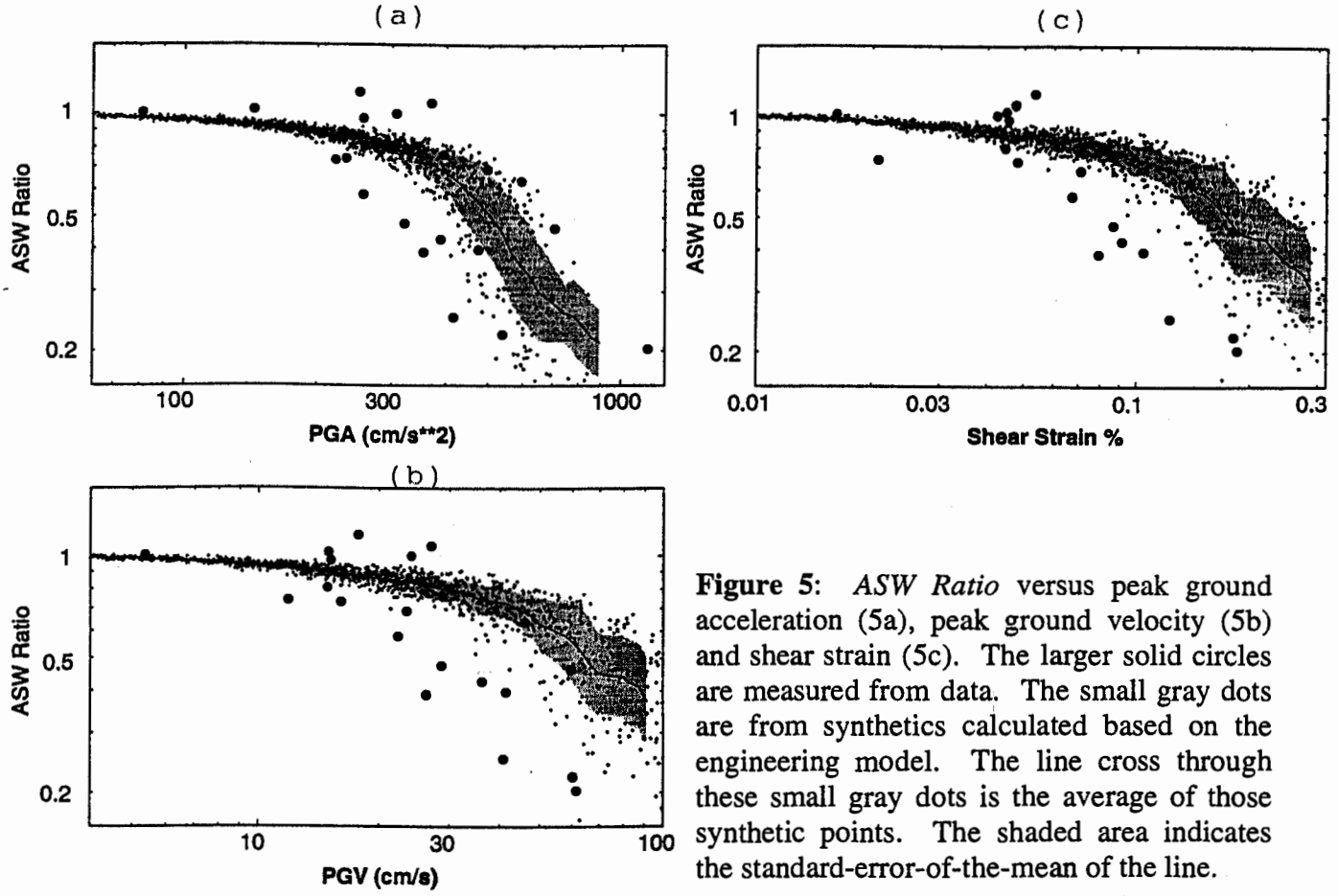

Figure 5: *ASW Ratio* versus peak ground acceleration (5a), peak ground velocity (5b) and shear strain (5c). The larger solid circles are measured from data. The small gray dots are from synthetics calculated based on the engineering model. The line cross through these small gray dots is the average of those synthetic points. The shaded area indicates the standard-error-of-the-mean of the line.

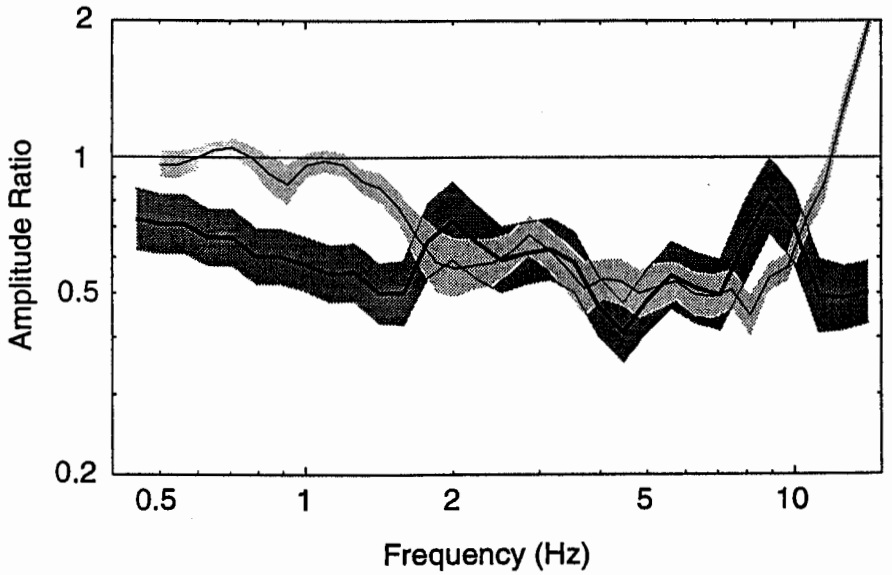

Figure 6: Ratio of strong to weak motion site response versus frequency averaged over 15 sediment sites we used. The thick line is from data and the thin line is from synthetics. The shaded area indicates the 95% confidence zone.

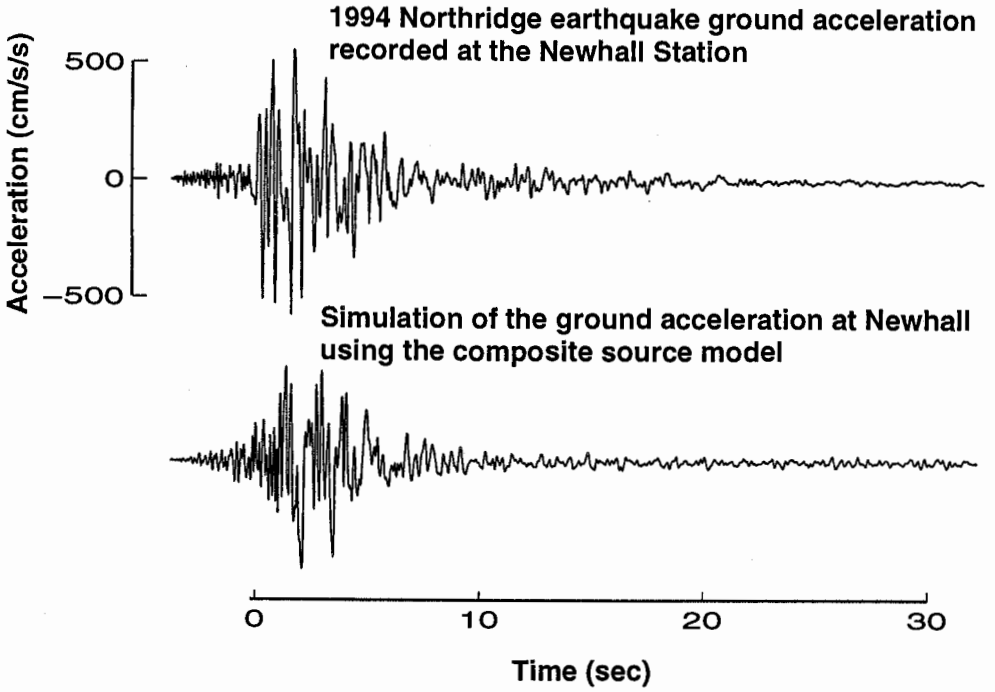

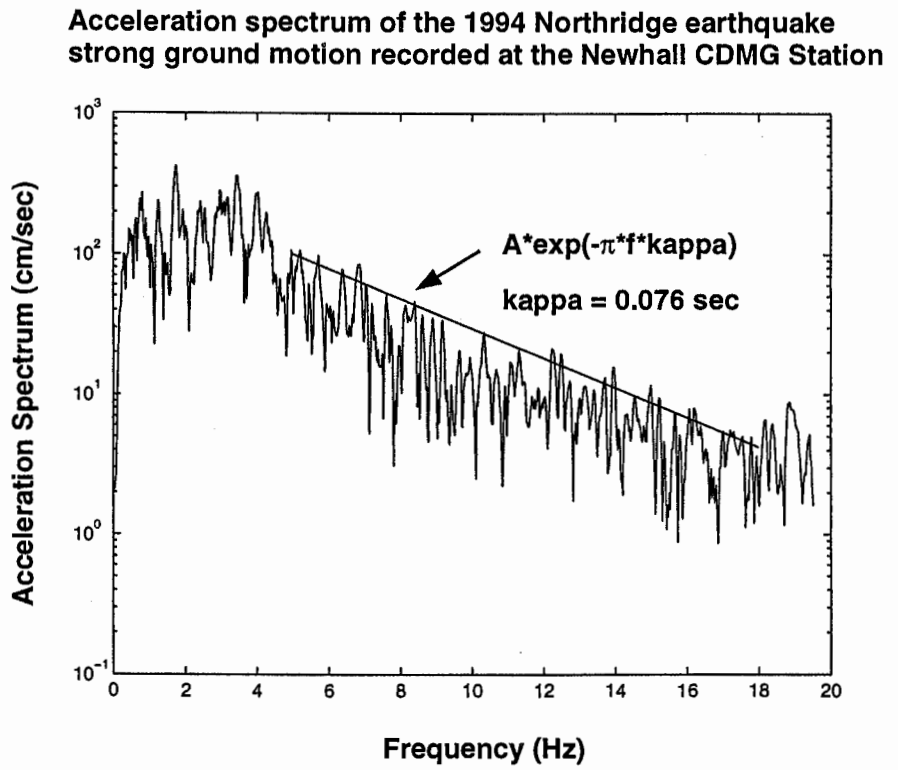

Figure 7. Top panel shows a comparison between an observed strong motion accelerogram and a synthetic one for the Northridge earthquake. The lower panel show the spectrum of the accelerogram and its kappa estimated from the spectral decay at high frequency.

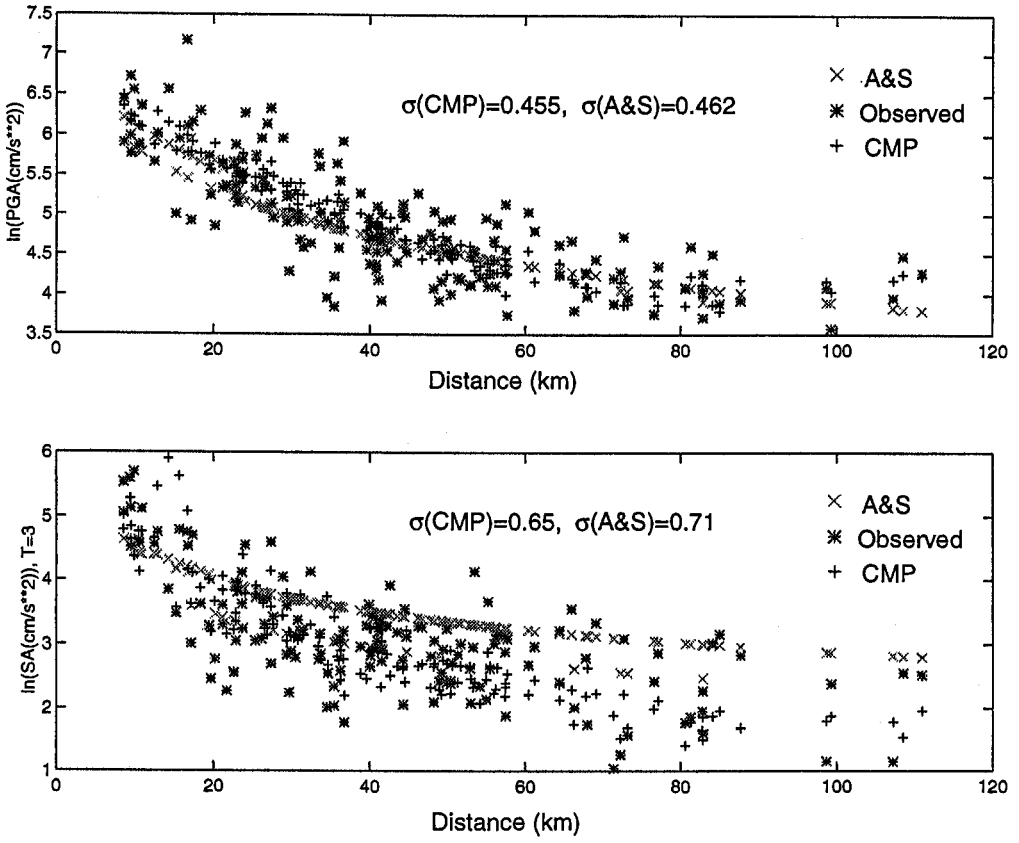

Figure 8. Comparison between observed and predicted peak ground motion parameters for the Northridge earthquake, 1994. The upper panel is for the peak ground acceleration and the low panel is for the spectra acceleration with 5% damping at 3 second period.

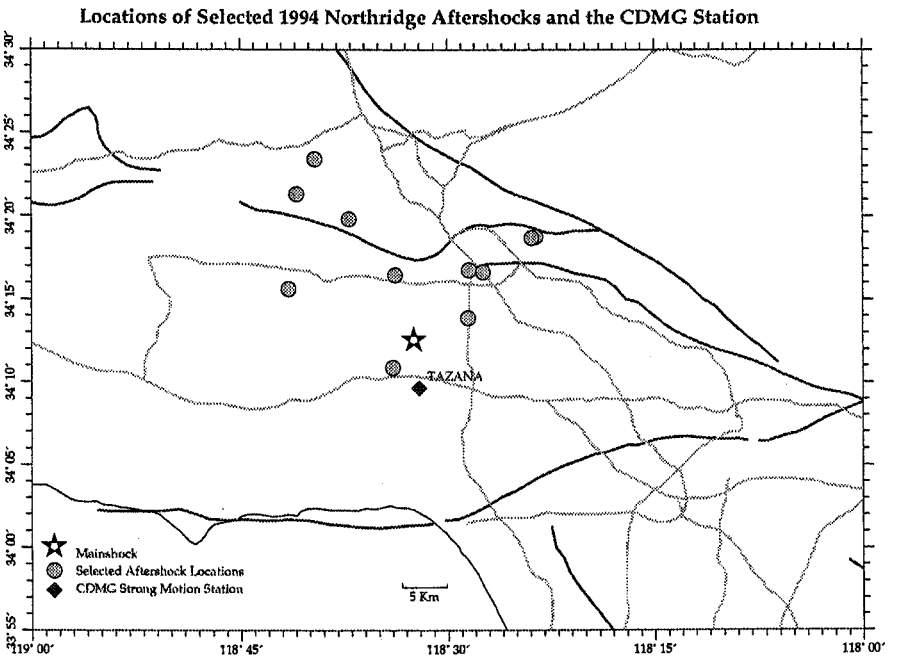

Figure 9. Map view of the Northridge aftershocks and station distribution used for this study.

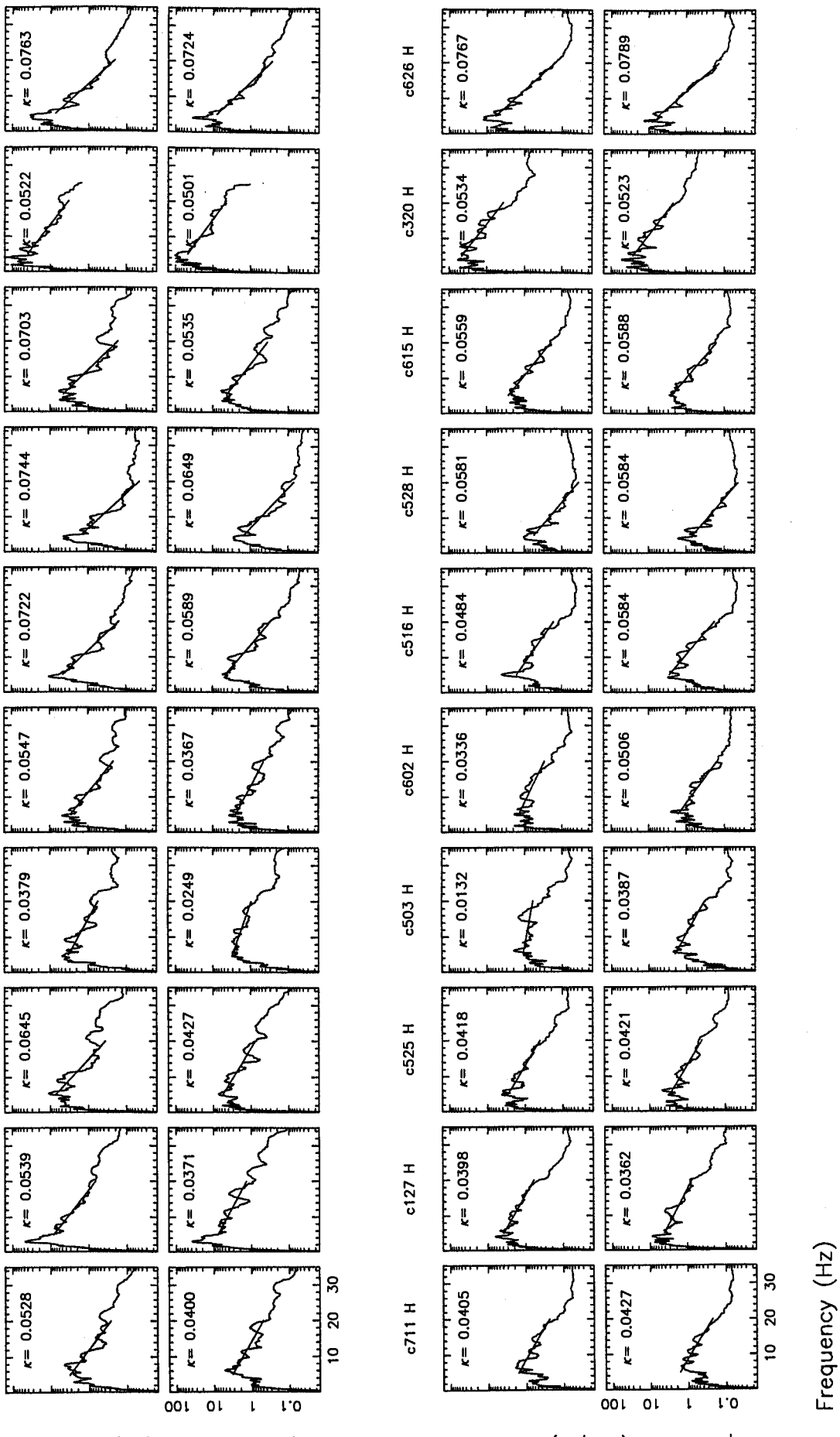

Figure 10: Acceleration spectra of the 10 aftershocks and their spectral fits that produce the individual κ measurements. These 10 aftershocks are recorded in both station NUR and CLU from Jan. 27, 1994 and July, 11, 1995 (CSMIP data report OSMS 96-06, Darragh et al., 1996).

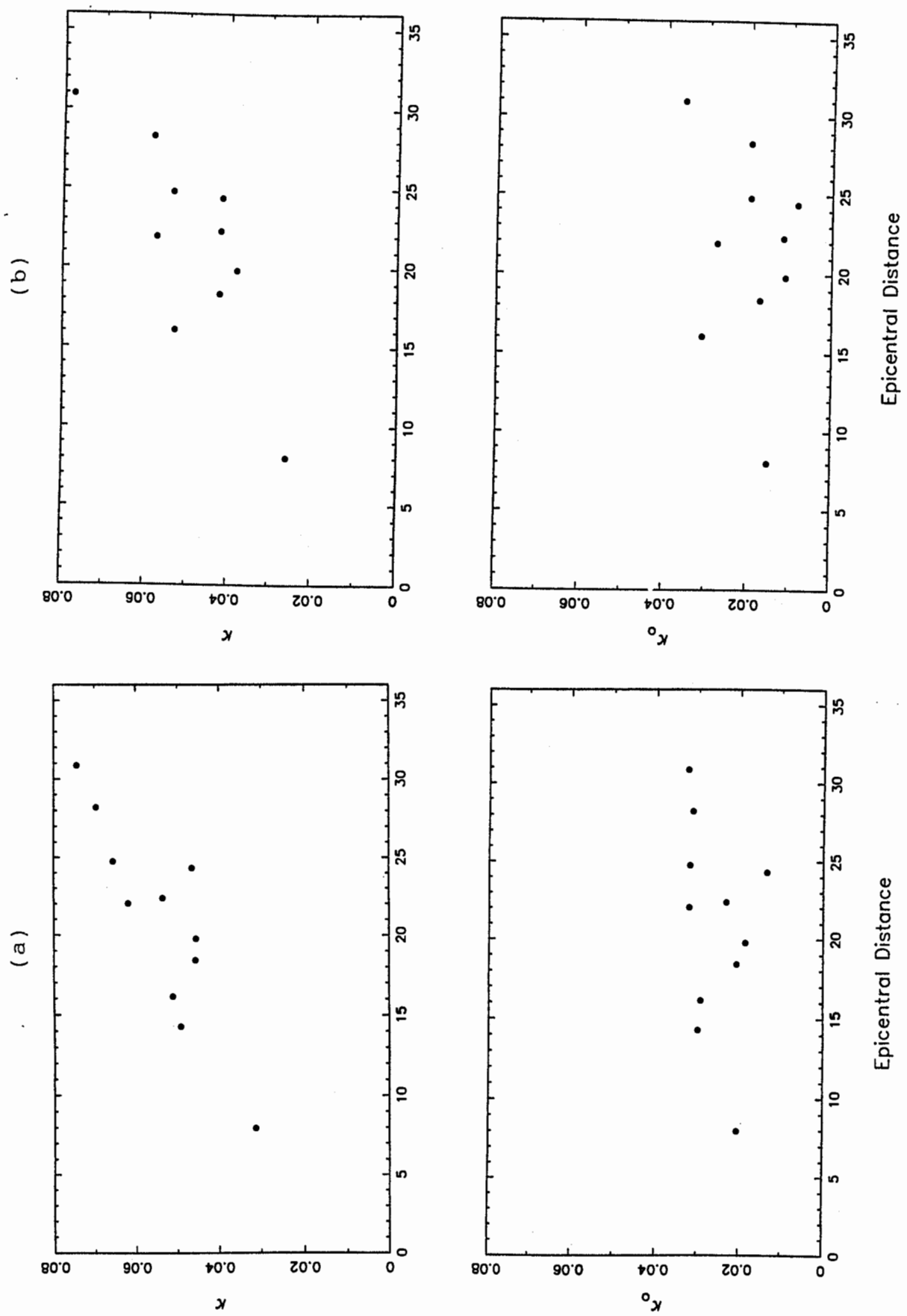

Figure 11: Estimated κ and κ_0 versus distance, (a) for station NUR; (b) for station CLU.

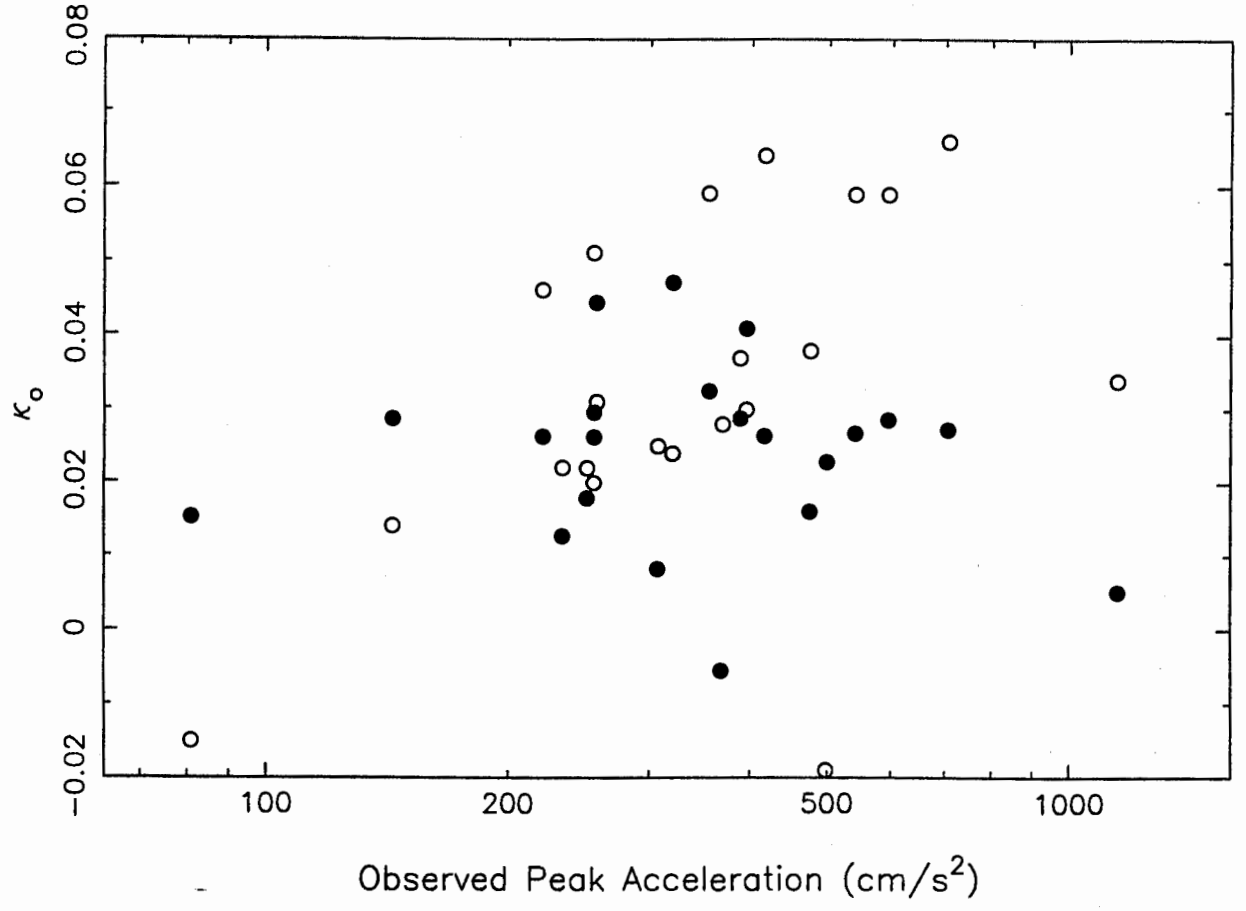

Figure 12: Estimated κ_o from strong motion stations (solid circle) and weak motion stations (open circle) versus observed PGA during the Northridge mainshock at these stations.

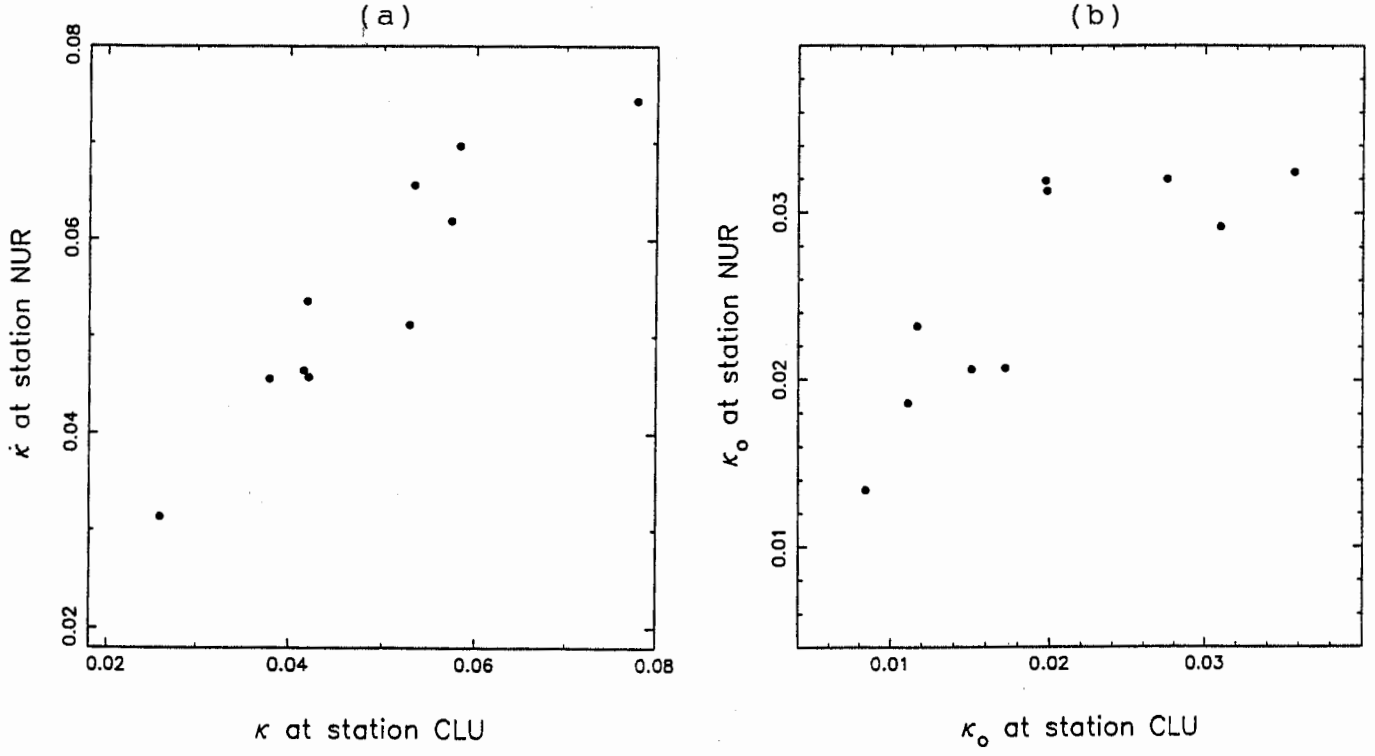

Figure 13: (a) Comparison of estimated κ between station NUR and CLU; (b) comparison of estimated κ_o between NUR and CLU.